Crater Creation on the Surface of Refractory Alloy Parts During Intense Pulsed Ion and Electron Beam Irradiation

V.A. Shulov[1], V.I. Engelko[2], I.V. Kovalev[2], G. Mueller[3]

[1]*Moscow Aviation Institute, Volokolamskoye chosse 4, Moscow 125993, Russia, Tel.: (7-095) 1584424, Fax: (7-095) 1582977, E-mail: shulovva@ mail. ru u*
[2]*Efremov Institute of Electro-physical Apparatus, 1 Sovietsky Avenue, Metallostroy, St. Peterburg 189631, Russia; Tel.: (7-812) 4627845, Fax: (7-812)4639812, E-mail: engelko@ sirius.niiefa.spb. ru*
[3]*Forschungszentrum Karlsruhe GmbH, Institut für Hochleistungsimpuls- und Mikrowellentechnik Postfach 640 D-76021 Karlsruhe Tel: +49 (0)7247-82 4669; Fax +49 (0)7247-82 4874l, E-mail: georg.mueller@ihm.fzk.de*

Abstract – The effect of intense pulsed ion and electron beam irradiation and various methods of the preliminary surface treatment on the crater creation process was examined using Auger electron spectroscopy, X-ray diffraction analysis, scanning electron spectroscopy, and optical metallography. The crater distribution density, sizes and shape, along with their microhardness and chemical composition inside and outside them were determined. The studied samples were made of bars, produced of the following refractory alloys: VT8M, VT9, VT18U, EP866sh, and EP718ID with the use of machining. The irradiation of these samples was carried out using TEMP and GESA accelerators under the crater creation regimes. Some of targets were also subjected to various treatments as grinding, polishing, diamond smoothing, surface plastic deformation, chemical etching, and oxidation prior to irradiating by intense pulsed ion and electron beams. As a result of these experiments, the most probable mechanisms of crater formation on the surface of refractory alloy targets were established. In order to reduce the negative effect of crater creation upon the properties of targets can be proposed to use the fine polishing when preparing the surface for the irradiation and to carry out the final ion and electron beam treatment at low energy density in a pulse (crater free irradiation.

1. Introduction

It is well known that crater creation on the solid surfaces, when irradiating them by intense pulsed, ion and electron beams (IPPIB and IPEB) [1–4] leads to the catastrophic deterioration of the property level (fatigue strength, oxidation resistance, salt corrosion resistance, etc.) of irradiated components. As a result, the study of crater creation mechanisms and the development of methods allowing to decrease the negative influence of already created craters upon the operating characteristics of irradiated components are the most important factors. The objective of the present paper is the study of such effects as the preliminary surface treatment and irradiation conditions (particularly, energy density in a pulse and number of pulses) on the crater creation process.

2. Experimental

The studied specimens were made of bars, produced of the following alloys and steels: VT8M (Ti-6Al-3.7Mo-0.2Fe-0.3Si), VT9 (Ti-7Al-3.8Mo-0.2Fe-2.5Zr-0.3Si), VT18U (Ti-6Al-3.4Mo-0.2Fe-4.5Zr-1.5Nb-0.25Si-3Sn), VT25U (Ti-7Al-2.5Mo-1.5W-0.2Fe-2.5Zr-0.25Si), EP866sh (Fe-2.1Ni-16.5Cr-1.6Mo-1W-0.3Nb-5.5Co-0.6Si), and EP718ID (Ni-33Fe-2.4Ti-16Cr-1.4Al-5.2Mo-3.5W-1.5Nb-0.6Mn-0.3Si) with the use of machining [5]. Furthermore, the super-pure monocrystals of Zr and Cr produced by chemical transport reaction methods were used as the special samples. The irradiation of these targets ($14\times7\times3$ mm^3) was carried out at the TEMP accelerator [6] and the GESA-1 accelerator [7]. The treatment at the TEMP accelerator was realized by carbon (70%) and protons under the following conditions: ion energy – 300 keV (E), pulse duration – 50 ns (τ), and the energy density in a pulse (w) as well as a number of pulses (n) were varied from $w = 0.3$ J·cm^{-2}, $n = 1$ up to $w = 3.3$ J·cm^{-2}, $n = 10$. The processing with the use of the GESA-1 accelerator was carried out under the following regimes: $E = 115$–120 keV, $\tau = 20$–40 μs, $w = 16$–55 J·cm^{-2}, $n = 1$–10 pulses. After the irradiation some targets were studied by Auger electron spectroscopy (AES), X-ray diffraction analysis, scanning electron microscopy (SEM), optical microscopy (OM), and microhardness (H_μ) measurements. Other irradiated specimens were subjected to vacuum annealing for 2 hours at the given operating temperature for each alloy, in particular, VT8M, VT9-500 °C; VT18U, VT25U-550 °C; EP866sh-600 °C, and EP718ID-650 °C. After completing the pointed heat treatment the studying cycle was repeated again. In this case it should be noted that some of targets were also subjected to various treatments as grinding, polishing, diamond smoothing, surface plastic deformation, chemical etching, and oxidation prior to irradiating by IPIB and IPEB. The crater distribution

density (ρ), their evarige linear size (D_{av}) and form along with the microhardness and chemical composition inside and outside them were determined during the performed studies. In addition to these studies, there were some prescratched samples, which were also irradiated and investigated.

3. Results and Discussion

The results of the performed investigations allow to divide all craters into several groups depending on the crater shape. They can be classified into the following types: round-shaped craters with the convex centre (Fig. 1, *a*) and the concave centre (Fig. 1, *b*); round-shaped multi-rings craters (Fig. 1, *c*); adjoining craters (Fig. 1, *d*); craters in the form of ellipse, crack and disk including also faceted and dent-shaped ones.

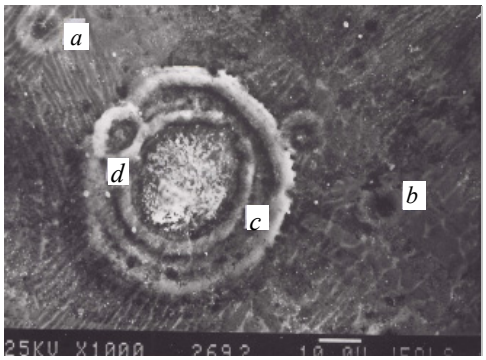

Fig. 1. SEM-micrograph of VT9 alloy surface treated by IPIB ($w = 2$ J·cm^{-2}, $n = 3$ pulses): *a*, *b* – round-shaped craters with the convex centre and the concave centre; *c* – round-shaped multi-rings craters; *d* – adjoining crater

Analysis of the results presented in Tables 1, 2 and published in [8–10] gives a possibility to trace the effect of irradiation conditions on the type, size, and distribution density of craters through the surface. It is obvious that the energy density (w) increase from 0.6 up to 1.7 J·cm^{-2} leads to the increase of the crater distribution density (ρ) from 0 up to 1100–1400 cm^{-2} after IPIB irradiation and from 0 up to 8–10 cm^{-2} as a result of the irradiation by IPEB with the energy density rise from 18 up to 32 J·cm^{-2}. The tendency to the decrease of ρ down to 200–500 cm^{-2} (IPIB) and 3–5 cm^{-2} (IPEB) and the growth of craters takes place with the further increasing w (1.8 → 2.6 J·cm^{-2}, IPIB) and (32 → 55 J·cm^{-2}, IPEB). However, a value of ρ is firstly increased with a rise of a pulses number ($n = 1$, 2, 3) and then it is decreased ($n = 5$–10). It is impossible to establish any dependence between ρ and n values if the energy density achieves high values of w ($w > 2.4$–2.6 J·cm^{-2}, IPIB and $w > 32$–36 J·cm^{-2}, IPIB). On the base of the fixed experimental results one more important conclusion can be made, that the formation of round-shaped and faceted craters occurs mainly when irradiation with the energy density of 1.5–2.2 J·cm^{-2} (IPIB) and 24–32 J·cm^{-2} (IPEB) and the creation of dent-shaped and faceted craters and cracks of dent-shaped and faceted craters and cracks takes place at very high values of the energy density (Fig. 2, *a*). The depth of the craters created by ion beams achieves 1–2 μm while the craters formed by electron beams have the depth of more, than 20–25 μm. The microhardness values near craters are significantly lower than the appropriate H_μ values, fixed on the "free" surface. H_μ (craters) is equal to H_μ (surface) only after the final annealing of irradiated samples.

Table 1. Distribution density and average size of craters formed on VT9 alloy specimen surface (Temp accelerator) and on EP866sh* steel specimen surafce (GESA-1 accelerator)

Irradiating conditions		ρ, cm^{-2}	D_{av}, μm
w, J/cm^2	n, pulses		
0.9	1	0	0
1.2	1	420 ± 20	5–10
1.5	1	580 ± 40	5–40
1.8	1	340 ± 30	15–50
2.4	1	260 ± 20	28–38
0.9	2	0	0
1.2	2	200 ± 20	5–7
1.5	2	1200 ± 200	5–7
1.8	2	1060 ± 200	10–40
0.9	3	0	0
1.2	3	1480 ± 200	5–15
1.5	3	1100 ± 200	5–15
1.8	3	1100 ± 200	10–40
0.9	5	0	0
1.2	5	920 ± 100	5–10
1.5	5	1100 ± 200	10–20
1.8	5	500 ± 100	25–60
2.4	5	260 ± 30	30–70
0.9	7	0	0
1.2	7	660 ± 70	10–40
1.5	7	900 ± 100	20–50
1.8	7	680 ± 50	20–60
2.4	7	460 ± 30	15–25
20*	1	0	0
26*	1	12 ± 2	90–130
32*	1	14 ± 4	80–150
40*	1	18 ± 3	120–130
45*	1	20 ± 4	100–120
50*	1	16 ± 4	130–180
55*	1	15 ± 4	120–170
20*	5	1–2	20–30
26*	5	5 ± 2	45–120
32*	5	6 ± 3	40–150
40*	5	5 ± 2	110–140
45*	5	6 ± 2	130–190
50*	5	5 ± 3	120–180
55*	5	4 ± 2	130–190

The chemical composition of craters being formed as a result of ion and electron beam irradiation with high values of the energy density can be similar to the chemical composition of the studied alloys. Only a great amount of carbon was determined into these craters. Meanwhile, if ion and electron beam processing was carried out at the average values of w, craters

contained a considerable amount of Mo, Zr, Si (titanium alloys) and Al, Mo, W (steels and nickel-base alloys).

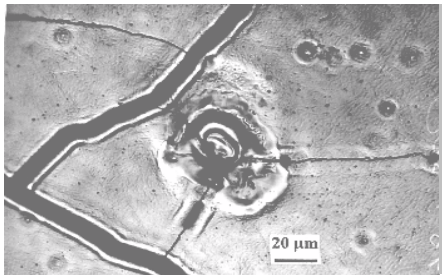

a

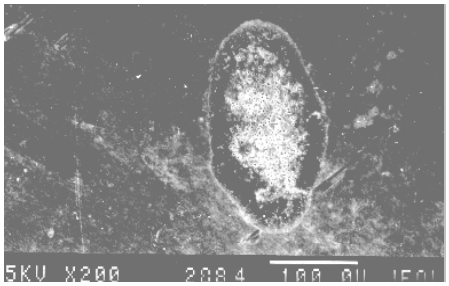

b

Fig. 2. SEM-micrograph of EP866sh steel (*a*) and VT9 alloy (*b*) surface treated by IPIB (w = 2 J·cm^{-2}, n = 3 pulses)

Moreover, it was revealed that some craters contained the elements, typical of a structural material of the cathode system, when the irradiation was realized by ion beams (for example, Sn, Fe, Ni etc.). It points to the fact of the of the cathode erosion under HPPIB irradiation effect, and when bombarding the already melted surface of targets by eroded particles. Table 1 illustrates the effect of the energy density on the average size of formed craters. The intensive growth of new phases (carbides, oxides, and oxicarbides of Sn, Zr, Mo, W, Si, Al) within craters with the changed composition is observed during the final annealing. It' s explained by the rise of microhardness within craters as a result of the vacuum annealing. In this case the formation of separate 1–20 μm-crystals cab be occurred within craters These crystals can have various forms (dendrites, cubic and pyramidal crystals, Fig. 2, *b*). The intensive growth of crystals depends on the different conditions of heat transfer at the craters boundaries and the high residual stresses near craters.

It' s evident, that the preliminary diamond smoothing and vacuum annealing of sample surfaces allow to obtain the "crater-free" surface when irradiating by using any energy density (Fig. 3, *a*). The surface of the similar prescatched samples after the irradiation contains craters however, they are concentrated along the scratch (Fig. 3, *b*) only after ion beam treatment.

Some results of the second stage of experiments are presented in Table 2 and Fig. 3.

Table 2. Effect of the initial surface treatment on the crater creation process during the irradiation by IPIB (VT9, VT18U, and VT8, w = 2 J·cm^{-2}, n = 1 pulse) and IPED (EP866sh, w = 32 J·cm^{-2}, n = 1 pulse)

Treatment	Crater density, ρ, cm^{-2}			
	VT8	VT9	VT18U	EP866sh
Grinding	290	320	270	35
Polishing	60	90	70	4
Deformation	480	460	420	45
Etching	450	500	430	7
Oxidation	420	380	410	6

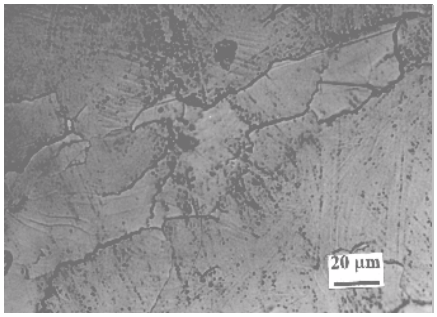

a

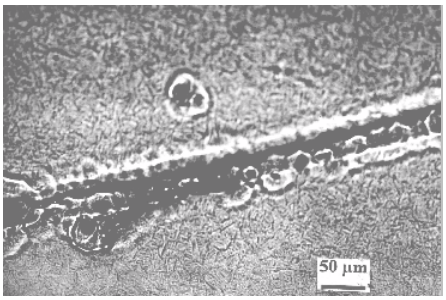

b

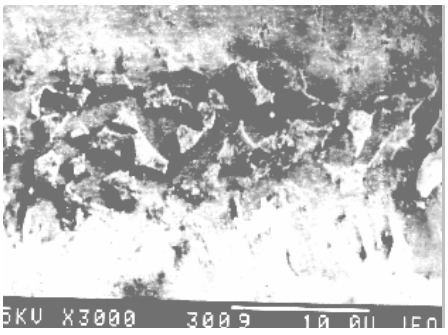

c

Fig. 3. SEM-micrographs of VT9 alloy (*a*) and VT25U alloy (*b*, *c*) specimen surface treated by IPEB (a – w=18 J·cm^{-2}, n = 3 pulses) and IPIB (b, c – w = 2 J·cm^{-2}, n = 3 pulses)

The craters were not observed along the scratch after electron beam treatment. One more important result of these experiments is the creation of craters, separate areas of which were not melted if the targets

were subjected to the preliminary diamond smoothing, final chemical etching and the irradiation by IPIB (Fig. 3, *c*). The irradiation of such specimens by IPEB exhibited the homogenious melt surface. The last differences are explained by more thickness of the surface layer modified with IPEB (20–30 μm) then with IPIB (1–2 μm). The craters were created even on the surface of the super-pure monocrystals of Zr and Cr produced by chemical transport reaction method as a result of the irradiation with IBEB (Fig. 4).

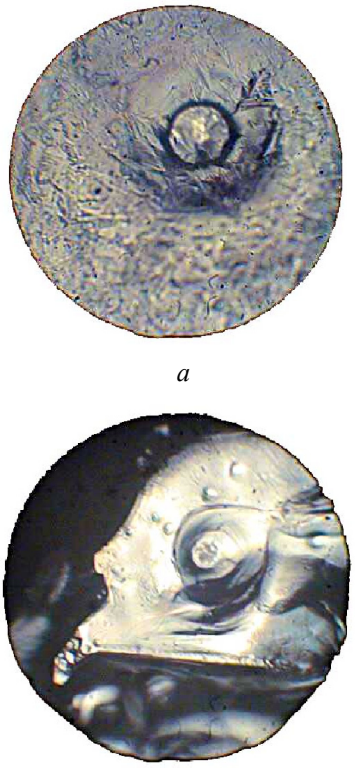

a

b

Fig. 4. Micrographs of Zr (*a*) and Cr (*b*) specimen surface treated by IPEB (w = 32 J·cm^{-2}, n = 1 pulse) x400

According to our experimental and published data [8, 9] the variety of the following crater creation mechanisms can be possible: the formation of a gas-plasma phase during the ablation of surface volatiles; the bombardment of the melted surface by the accelerator structure elements; and the availability of non-stable conditions during melting due to the difference in phase and chemical compositions, impurity distributions and dislocation densities of targets.

The formulated crater creation mechanisms give a possibility to propose a number of methods to reduce this surface phenomenon including: changes in ion accelerator electrode material (in particular, the target material instead of steel); target surface preparation such as fine polishing; follow-on beam treatment at low energy when the craters are not created; and the final implantation by heavy ions at low angles.

4. Conclusion

The major conclusions from this study can be summarized as follows:

1. Crater formation process takes place on the surface of solids during irradiation by IPIB and IPEB. This phenomenon is due to the cathode material erosion (technological factor) and the nonstability in the physical and chemical state of the irradiated surface.

2. In order to reduce the negative effect of crater formation upon the properties of targets can be proposed: changing the accelerator diode system material; to use the fine polishing when preparing the surface for the irradiation; to carry out the final IPIB and IPEB treatments at low energy density (crater-free irradiation); and to perform the final heavy ion implantation.

Acknowledgments

This research was supported by ISTC (project no. 975.2) and Education Ministry of Russia.

References

[1] G.E. Remnev and V.A. Shulov, J. of Laser and Particle Beams **11**, 707–741 (1993).
[2] V.A. Shulov, G.E. Remnev, F. Pelleran et al., J. of Surf. and Coat. Tech. **99**, 74–79 (1998).
[3] V.A. Shulov, N.A. Nochovnaya, G.E. Remnev, J. Proc. of the 8th Intern. Conf. on Titanium, UK **3**, 2126–2129 (1996).
[4] D.J. Rej, H.A. Davis, J.S. Olson et al., J. of Vac. Sci. Technol. **A15**(**3**), 1089–1092 (1997).
[5] K. Yatsui, J. of Laser and Particle Beams **7**, 733–746 (1989).
[6] G.E. Remnev, I.F. Isakov, M.S. Opekunov, J. of Surf. and Coat. Tech. **96**, 103–109 (1997).
[7] G. Mueller, G. Schumacher, D. Strauss et al., *in: Proc. of the Inter. Conf. "BEAMS-96"*, Prague, Vol. 1, 1996, pp. 267–272.
[8] V.A. Shulov, G.E. Remnev, I.G. Polykova etc., J. of Surface (Russia) **7**, 117–121 (1994).
[9] V.A. Shulov, G.E. Remnev, I.G. Polykova etc., J. of Surface (Russia) **11**, 24–29 (1995).